U. S. DEPARTMENT OF COMMERCE NATIONAL BUREAU OF STANDARDS

RESEARCH PAPER RP1447

Part of Journal of Research of the National Bureau of Standards, Volume 28, January 1942

ELASTIC PROPERTIES OF SOME ALLOY CAST IRONS

By Alexander I. Krynitsky and Charles M. Saeger, Jr.

ABSTRACT

Transverse-strength properties were determined on 1.2-in. diameter test bars made from three types of alloy iron heated, before casting, to the maximum temperatures of 1,400°, 1,500°, 1,600°, and 1,700° C. The bars were vertically cast, bottom-poured in green-sand molds, at a temperature of 100°, 150°, 200°, or 250° C above the liquidus. Total, plastic, and elastic deflection, modulus of rupture, relative moduli of elasticity, and total, plastic, and elastic resilience were determined, and the microstructure of the test bars was examined. Comparative values of four different relative moduli of elasticity relating to the same test bars but calculated by different methods are discussed. Comparison of transverse test properties of alloy and plain carbon irons is made.

CONTENTS

		Page
I.	Introduction	73
II.	Scope of investigation	73
	1. Metals used	74
III.	Foundry procedure	74
	1. Preparation of mold	74
	2. Melting	74
	3. Temperatures used and their measurement	74
IV.	General remarks concerning composition of transverse test bars	75
V.	Determination of transverse test properties	75
	1. Deflection	76
	2. Transverse strength	78
	3. Relative modulus of elasticity	81
	4. Resilience	85
	5. Hardness	88
VI.	Microscopic examination	89
VII.	Summary	92
VIII.	References	93

I. INTRODUCTION

A knowledge of the elastic properties of cast iron is important for its use in structural parts, such as piston rings, cylinder liners, etc. The present investigation is an extension to three types of alloy cast iron of a previous study [1] [1] of the elastic properties of three types of plain cast iron. The same procedure of melting and casting and the same methods of testing as those described in the previous paper were employed.

II. SCOPE OF INVESTIGATION

The research consisted in making transverse test bars 1.2 in. in diameter and 21 in. in length and testing these for transverse strength,

[1] Figures in brackets indicate the literature references at the end of this paper.

deflection, Brinell hardness, and microstructure. A universal testing machine of the hydraulic type of 50,000 lb capacity was used for transverse tests.

1. METALS USED

Three types of alloy cast irons were selected for this investigation: Iron *L*, a nickel-molybdenum high-silicon iron; iron *M*, a nickel-molybdenum-chromium, low-manganese, medium-silicon iron; and iron *N*, a nickel-molybdenum-chromium, high-manganese, high-silicon iron. The stock pig irons, *B* and *C* (table 1), used in the previous investigation were also employed in the present study. Stock iron *B* was employed in making heats of irons *M* and *N*, while stock iron *C* was employed for making heats of iron *L*.

TABLE 1.—*Chemical analysis of stock pig irons*

Iron	Total carbon	Silicon	Manganese	Phosphorus	Sulfur
	Percent	*Percent*	*Percent*	*Percent*	*Percent*
B	3.79	1.40	0.63	0.181	0.062
C	3.44	2.43	.77	.395	.050

III. FOUNDRY PROCEDURE

The foundry technique was similar to that used in the previous investigation.

1. PREPARATION OF MOLD

Molds for transverse test bars were made of a mixture of 8 parts of molding sand and 1 part of sea coal, tempered to approximately 7 percent of moisture. The mold cavities were faced with nongraphitic carbonaceous material of commercial origin.[2] The bars were bottom-poured in groups of four in a three-part vertical flask, and each flask contained two groups, that is, eight bars.

2. MELTING

Charges of 230 to 250 lb of iron, in a commercial magnesia crucible, were melted in a high-frequency induction furnace of the tilting type. When the charge of stock iron was melted, the metal was slagged off and necessary additions were made. First, open-hearth ingot iron was charged into the melt, and then other elements were added. Nickel was added in the form of nickel shot, whereas silicon, manganese, chromium, and molybdenum were added in the form of their respective ferro-alloys. The major portion of the ferro-silicon (about two-thirds of the total amount) was added after all other additions had been made. The elapsed time between the last addition of ferro-silicon and the pouring of a group of transverse test bars varied from about 4 minutes to 1 hour, depending upon the maximum heating and pouring temperatures employed.

3. TEMPERATURES USED AND THEIR MEASUREMENT

Each melt was heated to a predetermined maximum temperature of 1,400°, 1,500°, 1,600°, or 1,700° C (2,550°, 2,730°, 2,910°, or 3,090° F).

[2] Approximate analysis:

Volatile matter	4.0%
Fixed carbon	74.0%
Ash	22.0%

Each group of four bars was cast as a unit at a predetermined pouring temperature of 100°, 150°, 200°, or 250° C (210°, 300°, 390°, or 480° F), above the liquidus temperature of the iron investigated. Temperatures up to 1,600° C (2,910° F) were measured by a platinum to platinum-rhodium thermocouple and temperatures above 1,600° C (2,910° F) by an optical pyrometer. To determine the corrections to be applied to the readings of the optical pyrometer under these conditions, observations were taken simultaneously with both the thermocouple and the optical pyrometer in the temperature range of 1,400° to 1,550° C (2,550° to 2,820° F). These corrections were then plotted as a function of the temperature, and the curve extended up to 1,700° C (3,090° F). The thermocouple assembly used in measuring temperatures of molten cast iron was described in a previous paper [2].

IV. GENERAL REMARKS CONCERNING COMPOSITION OF TRANSVERSE TEST BARS

After completing the transverse tests, the bars were sampled for chemical analysis. The analytical data are summarized in table 2. Since the variation in pouring temperature did not appreciably affect the composition of heats, these data refer to the heats made at different maximum heating temperatures, the pouring temperature being constant.

The most consistent results were obtained with iron *L*, whereas a considerable fluctuation in composition was noticed for irons *M* and *N*, particularly in the content of silicon.

TABLE 2.—*Chemical analysis of cast iron bars of irons L, M, and N, heated to different maximum temperatures and poured at 1,350° C*

Iron	Maximum heating temperature	Chemical analysis									
		Carbon			Si	Mn	P	S	Ni	Cr	Mo
		Total	Graphitic	Combined							
	°C	%	%	%	%	%	%	%	%	%	%
L	1,400	3.38	2.82	0.56	2.35	0.63	0.39	0.05	1.04	-------	0.72
	1,500	3.33	2.79	.54	2.34	.70	.39	.05	1.05	-------	.76
	1,600	3.33	2.75	.58	2.39	.71	.39	.04	1.08	-------	.71
	1,700	3.23	2.62	.61	2.32	.72	.40	.04	1.01	-------	.75
M	1,400	3.16	2.43	.73	1.84	.43	.14	.03	1.57	0.27	.98
	1,500	3.12	2.37	.75	2.02	.45	.15	.03	1.60	.24	.77
	1,600	3.04	2.33	.71	2.02	.47	.14	.04	1.59	.24	.76
	1,700	3.14	2.42	.72	2.23	.53	.15	.04	1.67	.28	.86
N	1,400	2.83	2.10	.73	2.59	.89	.13	.04	1.24	.21	1.20
	1,500	3.06	2.46	.60	2.76	1.04	.13	.04	1.27	.21	1.09
	1,600	2.82	2.13	.69	2.75	.99	.13	.04	1.23	.21	1.22
	1,700	2.88	2.16	.72	2.70	.99	.12	.04	1.24	.21	1.17

V. DETERMINATION OF TRANSVERSE TEST PROPERTIES

The term "elastic properties" in this paper connotes those complex properties that determine the behavior of cast iron under load and, more specifically, under transverse bending load.

1. DEFLECTION

It is well known that the determination of the elastic properties of cast iron is complicated by the fact that even low stresses produce plastic as well as elastic deformation.

The method used by the National Bureau of Standards to measure deflection in cast-iron bars has been described elsewhere [1, 3]. A brief outline for the reader's convenience is as follows: As shown in figure 1, a rubber band, *B*, is stretched tightly along the length of the bar, *A*, and is held in position by two clamps, *C*. Metal strips on the inner surface of the clamps keep the rubber band near to, but not in contact with, the surface of the bar at all times. The 18-in. spacing between the two clamps is the same as that between the supports for the bar in the testing machine. A small piece of paper, *D*, is cemented to the surface of the bar midway between the clamps, *C*, and the upper edge of this piece of paper serves as a reference mark.

In conducting the test, the bar is placed in the testing machine (fig. 2) and a micrometer-telescope, *E* (fig. 1), mounted at a distance of 20 in. from the bar, is used to measure the distance between the lower edge of the rubber band and the reference mark. The rubber band clamped to the bar at the two supports remains practically straight, so that the displacement of the reference mark relative to the band is a measure of the center deflection of the loaded bar. A similar measurement after the load has been removed indicates the permanent set at the center.

After a test bar, *A*, was mounted in the testing machine and adjusted until the rubber band, *B*, was in the horizontal plane through the neutral axis of the bar, a load of 50 lb was applied and the distance between the lower edge of the rubber band and the reference mark was determined and used as the zero reading. This load was sufficient to seat the bar firmly. The deflection of the bar was then measured as it was loaded in a series of steps of 100 or 200 lb each. After the load had reached 1,000 lb, each application of load was followed by unloading to the original 50-lb load, and the permanent set in the unloaded bar was determined. The total deflection at the breaking load and the "set" of each bar under increasing step loadings were determined, and the elastic deflection was taken as the difference between the total and the plastic deflection for each load. In each group of four bars (poured at the same temperature), two were tested by the step loading and unloading method while the two companion bars were progressively loaded to failure, without unloading between successive loads. No difference in the breaking loads and the load-deflection curves, which could be ascribed to the mode of loading, was observed.

As shown in table 3, there is no definite relation between the ultimate total, as well as the ultimate elastic deflections and maximum heating and pouring temperatures. The ultimate total, elastic, and plastic deflections are considerably higher for irons *M* and *N* than for iron *L*. From table 3 and the data obtained in the previous investigation it may be noted that the ultimate total, elastic, and plastic deflections for plain carbon irons (irons *A*, *B*, and *C*) and alloy irons (irons *L*, *M*, and *N*) range as shown in table 4.

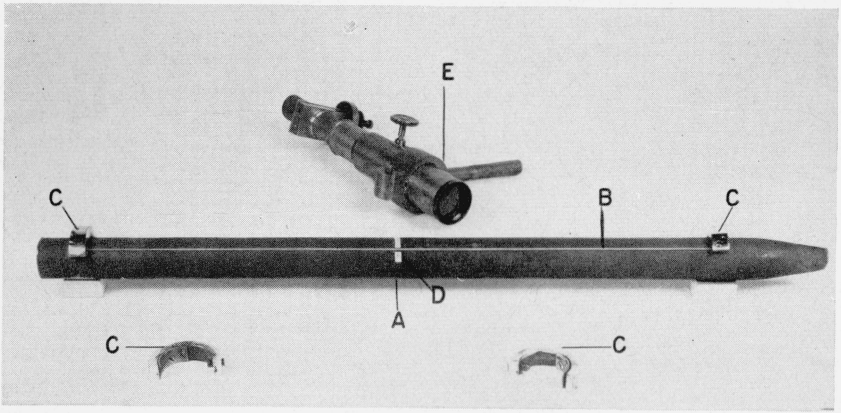

FIGURE 1.—*Apparatus for measuring deflection of cast-iron bars under transverse loading.*

A, Cast-iron bar; *B*, Rubber band; *C*, Clamps; *D*, Reference mark; *E*, Micrometer telescope.

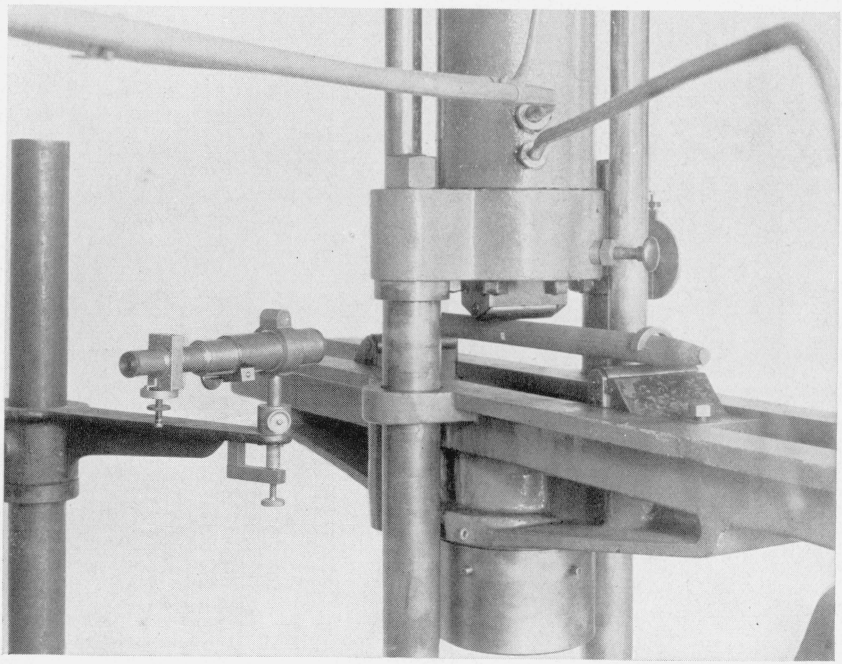

FIGURE 2.—*Test bar mounted in the 50,000 lb testing machine.*

Micrometer-telescope support is independent of the testing machine.

TABLE 3.—*Transverse breaking strength, modulus of rupture and ultimate total and elastic deflections* [1]

Iron	Pouring temperature	Transverse breaking strength of metal heated to—				Modulus of rupture of metal heated to—				Ultimate total deflection of metal heated to—				Ultimate elastic deflection of metal heated to—			
		1,400° C	1,500° C	1,600° C	1,700° C	1,400° C	1,500° C	1,600° C	1,700° C	1,400° C	1,500° C	1,600° C	1,700° C	1,400° C	1,500° C	1,600° C	1,700° C
	°C	lb	lb	lb	lb	lb/in.²	lb/in.²	lb/in.²	lb/in.²	in.	in.	in.	in.	in.	in.	in.	in.
L	1,400	----	2,440	2,590	2,640	----	64,800	68,700	69,900	----	0.22	0.24	0.22	----	0.20	0.20	0.19
	1,350	2,630	2,520	2,650	2,600	69,900	66,800	70,300	68,900	0.24	.21	.24	.21	0.20	.18	.21	.18
	1,300	2,730	2,620	2,760	2,830	72,300	69,600	73,100	75,000	.24	.22	.26	.22	.21	.19	.21	.18
	1,250	2,310	2,630	----	2,640	61,300	69,800	----	72,700	.22	.21	----	.22	.19	.19	----	.19
M	1,450	----	3,390	3,030	2,980	----	89,900	80,400	78,900	----	.36	.30	.31	----	.26	.23	.23
	1,400	3,190	3,180	3,250	3,111	84,600	84,500	86,200	82,000	.32	.31	.33	.31	.24	.24	.24	.23
	1,350	3,350	3,140	3,470	3,290	88,900	83,200	92,100	87,200	.34	.30	.36	.33	.24	.23	.26	.25
	1,300	3,430	3,360	3,140	3,220	91,100	89,200	83,300	85,500	.32	.35	.33	.31	.24	.26	.24	.24
	1,250	3,340	----	----	----	88,800	----	----	----	.34	----	----	----	.24	----	----	----
N	1,450	----	3,200	3,500	3,420	----	85,000	92,900	90,800	----	.31	.33	.30	----	.24	.25	.23
	1,400	3,400	3,290	3,690	3,520	90,200	87,300	97,800	91,600	.32	.31	.34	.30	.24	.25	.26	.23
	1,350	3,510	3,430	4,060	4,030	93,200	91,100	107,700	106,900	.32	.33	.37	.34	.24	.25	.28	.27
	1,300	3,550	3,610	3,960	3,720	94,100	95,800	105,200	98,700	.32	.33	.37	.33	.25	.26	.28	.25

[1] The values presented in this table are averages of values for a group of 4 bars cast at the same pouring temperature.

TABLE 4.—*Ultimate deflections and proportion of plastic deflection to the total deflection at fracture for alloy and plain carbon cast irons*

	Alloy irons			Plain carbon irons		
	L	*M*	*N*	*A*[1]	*B*[1]	*C*[1]
	Ultimate deflection (inches)					
Total	0.21 to 0.26	0.30 to 0.36	0.30 to 0.37	0.18 to 0.24	0.25 to 0.30	0.20 to 0.28
Elastic	.18 to .21	.23 to .26	.23 to .28	.15 to .18	.17 to .19	.16 to .21
Plastic	.02 to .05	.07 to .10	.07 to .09	.03 to .06	.08 to .11	.04 to .07
	Proportion of plastic deflection to the total deflection at fracture (percent)					
	9 to 19	23 to 28	23 to 24	17.0 to 25.0	32.0 to 37	20.0 to 25.0

[1] Iron *A* contains: Total C, 3.44 percent; Si, 1.40 percent; Mn, 0.15 percent; P, 0.46 percent; S, 0.02 percent. Chemical analyses of irons *B* and *C* are given in table 1.

Table 4 indicates that the ultimate elastic deflections obtained for alloy iron *L* are practically equivalent to those of plain carbon irons *A*, *B*, and *C*. However, the total plastic deflection of alloy iron *L* was somewhat inferior to those of the plain carbon irons *B* and *C*. The highest values of total and elastic deflections were observed for alloy irons *M* and *N*, whereas the highest values of plastic deflection were associated with plain carbon iron *B*. If the proportion of plastic deflection to the total deflection at fracture is considered as an index of rigidity of cast iron, then iron *L* is the most rigid and iron *B* the least rigid. The rigidities of irons *M*, *N*, *A*, and *C* are almost equal.

All the results of this investigation confirm the conclusions drawn from the previous study [1] with regard to the total, plastic, and elastic deflection curves obtained by the method just described, that is, the total and plastic deflection curves are continuous curves inclining progressively toward the deflection axis. The elastic-deflection curve is a straight line in its lower portion, but at approximately three-fifths of the breaking load, it inclines toward the deflection axis. Typical load-deflection curves for the irons investigated are shown in figure 3. All transverse tests were made with a universal testing machine of the hydraulic type of 50,000 lb capacity, the rate of loading corresponding to 0.12 in. per minute travel of the free cross head of the testing machine. According to an ASTM specification,[3] the error for loads within the loading range of a testing machine shall not exceed 1 percent. Since the error of the machine for loads smaller than 1,000 lb exceeds 1 percent, only the total deflections were measured at the loads of 400, 600, 800, 1,000 lb, etc., and no plastic and elastic deflections were determined at loads less than 1,000 lb. Consequently, curves corresponding to the loads below 1,000 lb are not shown in figure 3. It may be stated, however, that in most of the cases observed the initial portions of the load-total deflection diagrams (for loads of 200 to 1,000 lb) appeared to be continuous smooth curves. This was particularly true of the alloy irons.

2. TRANSVERSE STRENGTH

It may be noted in table 3 that the transverse breaking strengths for iron *L* range from 2,310 to 2,830 lb/in.^{2}, iron *M* from 2,980 to

[3] Specification E4-36, Am. Soc. Testing Materials, Standards, pt. 1, Metals, p. 774 (1939).

3,470 lb/in.^{2}, and iron *N* from 3,200 to 4,060 lb/in.^{2} In accordance with ASTM classification,[4] these irons would fall in the following classes: Iron *L*, 35–40; iron *M*, 50; and iron *N*, 50–60 or higher.

The higher strength of irons *M* and *N*, as compared with iron *L*, probably is due to their higher nickel content and more particularly to the presence of chromium. The low carbon, high manganese, and molybdenum contents of iron *N* appear to account for the higher strength as compared to iron *M*. This high strength was obtained in spite of the larger silicon content present in iron *N*. As shown in figure 4, the maximum heating temperature had no effect on the transverse strength of irons *L* and *M*, but the strength of iron *N* was found to be somewhat higher for the maximum heating temperature of 1,600° and 1,700° C (2,910° and 3,090° F) than for 1,400° and 1,500° C (2,550° and 2,730° F). In general, however, lower pouring tem-

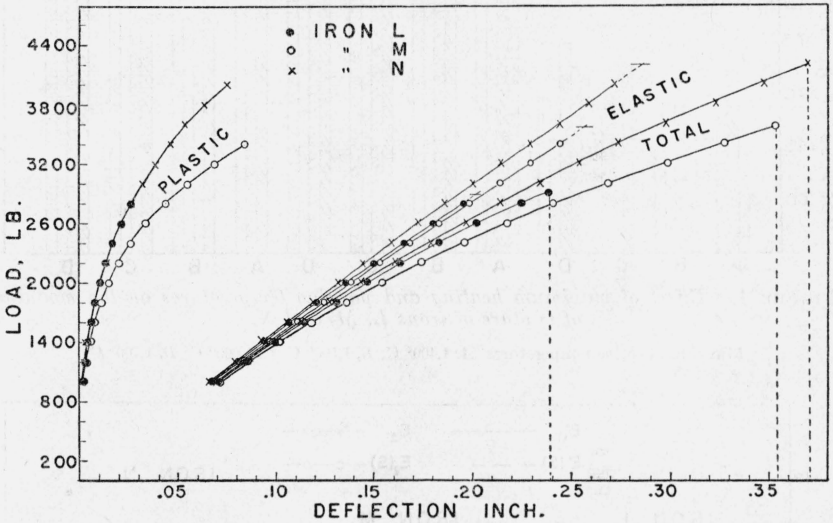

FIGURE 3.—*Typical plastic-, elastic-, and total-deflection curves of irons L, M, and N.*

peratures, ranging from 100° to 150° C above the liquidus, tend to produce stronger irons.

It is very probable that the effect of maximum heating temperature on the physical properties of these irons was, to a certain degree, masked by the variation in chemical analysis and the time of making the last addition of silicon to the melt before pouring.

In comparing the transverse strengths of alloy irons with those of plain carbon irons *A*, *B*, and *C*, previously studied, it may be stated that the strongest plain carbon iron, *A*, is equivalent to the nickel-molybdenum iron, *L*. The beneficial effect of increasing the maximum heating temperature on the transverse strength was more pronounced for plain carbon irons than for alloy irons.

The effect of pouring temperature for both types of iron was about the same, that is, the transverse strength tended to increase with a decrease of pouring temperature.

[4] Specifications A 48-36, Am. Soc. Testing Materials, Standards, pt. 1, Metals, p. 482 (1939).

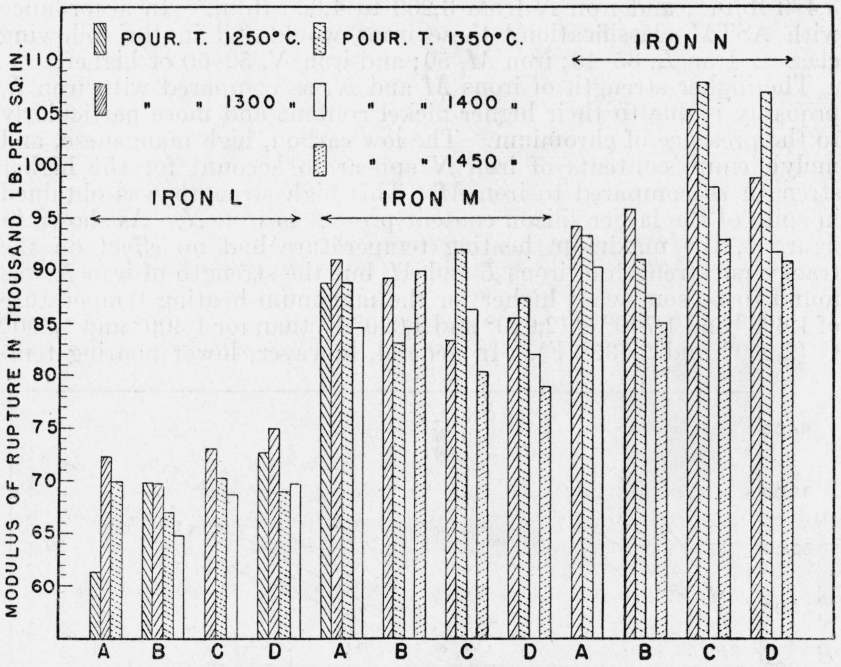

FIGURE 4.—*Effect of maximum heating and pouring temperatures on the modulus of rupture of irons L, M, and N.*

Maximum heating temperatures *A*, 1,400° C; *B*, 1,500° C; *C*, 1,600° C; *D*, 1,700° C.

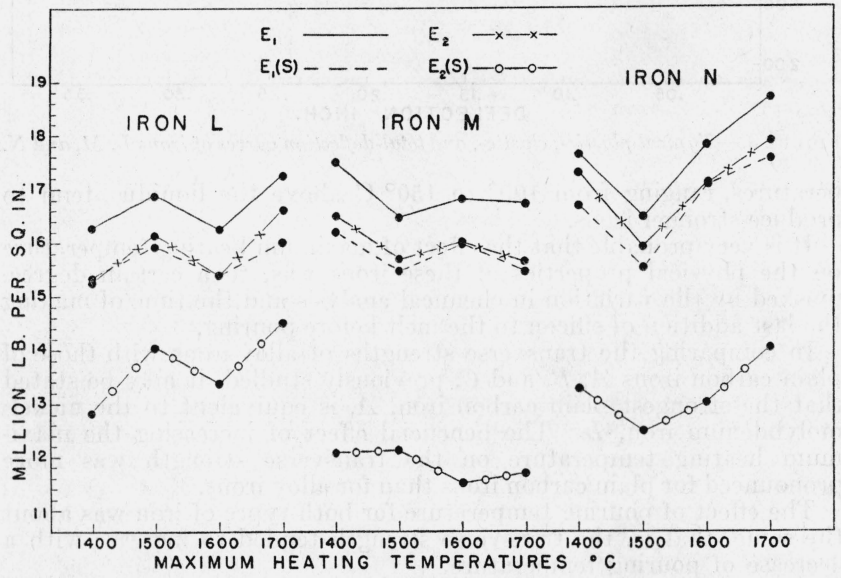

FIGURE 5.—*Comparative values of moduli of elasticity of irons L, M, and N calculated by different methods.*

3. RELATIVE MODULUS OF ELASTICITY

In the American Foundrymen's Association Cast Metals Handbook, the term "modulus of elasticity," as applied to gray iron, generally means the relative stiffness of the irons under the particular conditions of loading. In the previous and in this investigation, the term "relative modulus of elasticity" is used in place of "modulus of elasticity." Different relative moduli of elasticity were calculated from the data obtained in this investigation, as follows:

E_1=Relative modulus computed by simple beam theory from slope of straight line through elastic load-deflection curve at 1,200 lb.

$E_1(S)$=Relative modulus computed from slope of secant to load-total deflection curve at 1,200 lb.

E_2=Relative modulus computed from slope of secant through elastic load-deflection curve at failure.

$E_2(S)$=Relative modulus computed from slope of secant to load-total deflection curve at failure.

The average values of different moduli of elasticity of irons *L*, *M*, and *N* obtained at different maximum heating and pouring temperatures are given in table 5. In order to compare the different moduli of elasticity, values corresponding to 1,350° C pouring temperature are plotted for different maximum heating temperatures (fig. 5).

From the figures it may be observed that the relative moduli of elasticity are arranged according to their numerical values in the following order: the values for E_1 are the highest and for E_2 (S) the lowest; E_2 and E_1 (S) values are comparatively close together; and in general, there is a small difference between E_1, E_2, and E_1 (S) values, but E_2 (S) is considerably lower. When a similar plotting is made for four different moduli of elasticity of the plain carbon irons, *A*, *B*, and *C*, previously investigated, the results obtained are similar to those just described for the alloy irons.

As has been mentioned, in the determination of the relative moduli of elasticity, E_1 and E_2, it is necessary to define complete load-deflection curves by means of stepwise loading and unloading. This is a rather tedious procedure and requires a great deal of time. It was thought, therefore, that the determination of the relative modulus of elasticity would be simplified if a definite relation could be established between the relative modulus of elasticity, E_1, and the relative secant modulus of elasticity, E_1 (S), computed for the same load. With this thought in mind, calculations were made to determine the ratios between moduli E_1 and E_1 (S) for all transverse test bars investigated, the load of 1,200 lb being adopted as a minimum load for these calculations. The data obtained indicate that the $E_1/E_1(S)$ ratios were around 1.060.

It seems, therefore, that for practical purposes for the irons investigated, it may be assumed that

$$E_1 = E_1\,(S) \times 1.060.$$

It has been found, however, that this assumption can be applied only to the group of alloy irons under present study. When similar calculations were made for the plain carbon irons, *A*, *B*, and *C* previously reported, it was observed that the $E_1/E_1(S)$ ratios were quite different and extremely irregular.

TABLE 5.—*Relative moduli of elasticity* ($lb/in.^2 \times 10^6$)

Iron	Pouring temperature	Modulus of elasticity, E, at load of 1,200 lb, of metal heated to—				Secant modulus of elasticity at load of 1,200 lb, $E_1(S)$, for metal heated to—				Ultimate modulus of elasticity, E_2, for metal heated to—				Ultimate secant modulus of elasticity, $E_2(S)$, for metal heated to—			
		1,400° C	1,500° C	1,600° C	1,700° C	1,400° C	1,500° C	1,600° C	1,700° C	1,400° C	1,500° C	1,600° C	1,700° C	1,400° C	1,500° C	1,600° C	1,700° C
	°C																
L	1,400	----	16.25	15.85	17.68	----	15.14	14.81	16.54	----	14.92	15.14	16.71	----	12.76	13.06	14.27
	1,350	16.27	16.90	16.24	17.25	15.35	15.91	15.41	16.00	15.26	16.13	15.39	16.62	12.83	14.05	13.39	14.51
	1,300	16.56	17.40	16.15	17.55	15.61	16.29	15.19	16.54	15.49	16.12	15.15	16.57	13.00	14.18	12.92	14.47
	1,250	16.80	17.81	----	18.00	15.86	16.39	----	16.97	15.35	16.83	----	17.00	12.68	14.67	----	14.77
M	1,450	----	16.65	16.91	15.89	----	15.52	16.02	14.60	----	15.74	16.09	15.49	----	11.28	12.27	11.67
	1,400	16.81	16.82	17.08	16.46	15.61	15.66	15.89	15.37	15.98	15.84	16.49	15.52	12.03	11.66	11.97	11.94
	1,350	17.50	16.48	16.82	16.72	16.20	15.45	15.99	15.47	16.51	15.71	16.01	15.67	12.08	12.13	11.52	11.71
	1,300	17.45	----	16.60	17.08	16.54	15.40	15.57	16.03	16.52	15.36	15.83	16.23	12.05	11.32	11.79	12.37
	1,250	17.54	----	----	----	16.79	----	----	----	16.69	----	----	----	12.07	----	----	----
N	1,450	----	16.29	17.27	17.63	----	15.12	16.19	16.97	----	15.95	16.36	17.37	----	12.77	12.92	13.83
	1,400	17.62	16.41	17.15	18.03	16.30	15.28	16.38	16.80	16.59	15.91	16.82	17.71	12.94	12.46	13.16	14.31
	1,350	17.64	16.46	17.81	18.74	16.70	15.52	17.11	17.55	17.30	15.91	17.09	17.87	13.29	12.48	13.01	14.03
	1,300	17.99	17.41	17.93	18.36	16.96	16.23	16.61	17.09	17.26	16.69	17.15	17.52	13.37	13.03	12.92	13.65

[1] The values presented in this table are averages of values for a group of 4 bars cast at the same pouring temperature.

In figure 6 these ratios are plotted for the transverse test bars of both plain carbon and alloy irons against moduli E_1. It may be seen that most $E_1/E_1(S)$ ratios of alloy irons approach very close to the value 1.060, whereas the same ratios applied to plain carbon irons give widely scattered values. It already has been mentioned that for the testing machine used in this and previous investigations, the initial portion (for loads less than 1,000 lb) of the load–total-deflection

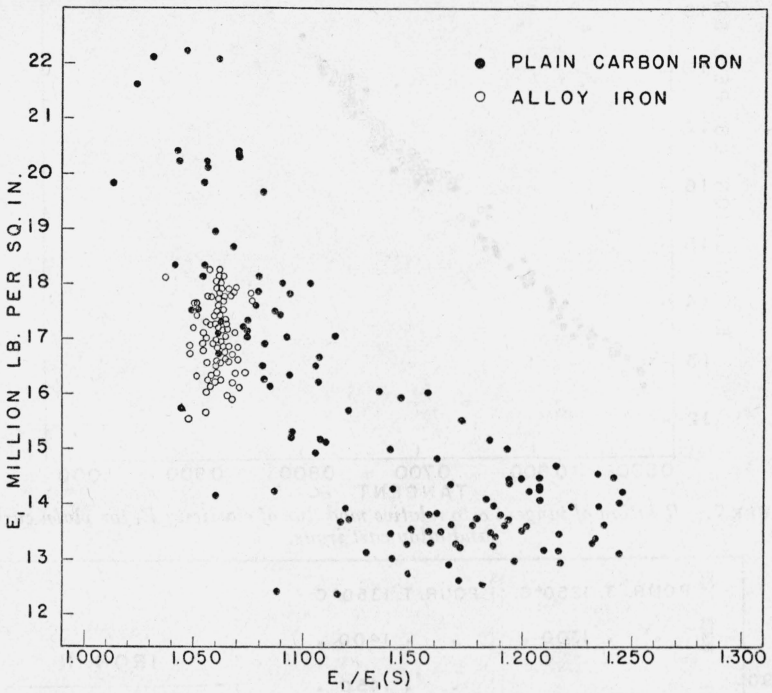

FIGURE 6.—*Relation of $E_1/E_1(S)$ and relative modulus of elasticity, E_1, for plain carbon and alloy cast irons.*

diagram cannot be regarded as accurate. On the other hand, the statement has been made that actually these initial portions of most diagrams appeared to be continuous smooth curves. In view of this fact it was thought that an approximate relationship can probably be obtained between the initial slope of these curves and the modulus E, if the tangent of angle α, at which the initial portion of the load–total-deflection curve is inclined at its origin towards the deflection axis, is plotted[5] against modulus E_1. Thus, the angles, α, of the continuous smooth curves obtained for the transverse test bars of plain carbon and alloy irons were measured by means of a protractor, and tangents of these angles were plotted against moduli E_1 (fig. 7).

The highest values of E_1 were obtained with iron L heated to a maximum temperature of 1,700° C, but in general (fig. 8), no definite relation was established between E_1 and the maximum heating tem-

[5] Method of plotting adopted after Carl Benedicks, *Om de fasta lösningarnas elasticitet*, Jernkontorets Ann. **124**, 225 (1940); also, *The elastic modulus of solid solutions*, Metallurgist, **20** (1941).

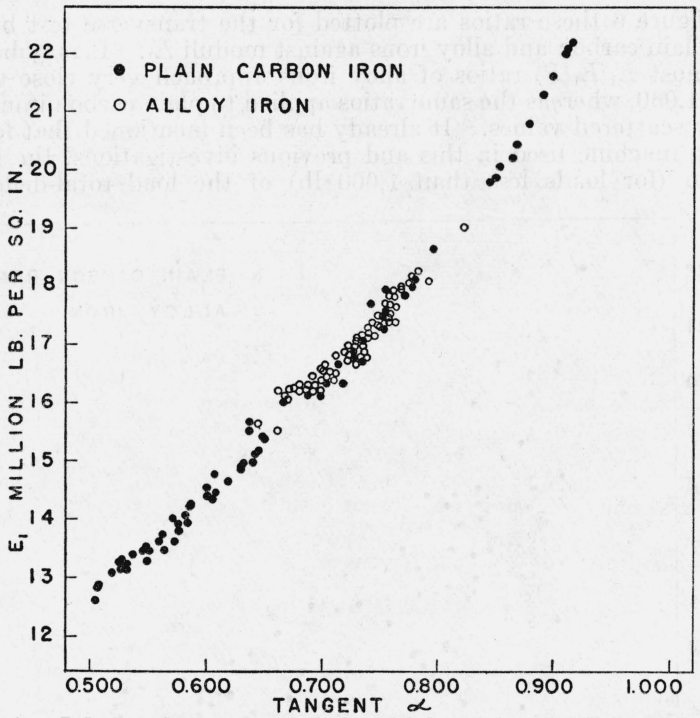

FIGURE 7.—*Relation of tangent α to relative modulus of elasticity E_1 for plain carbon and alloy cast irons.*

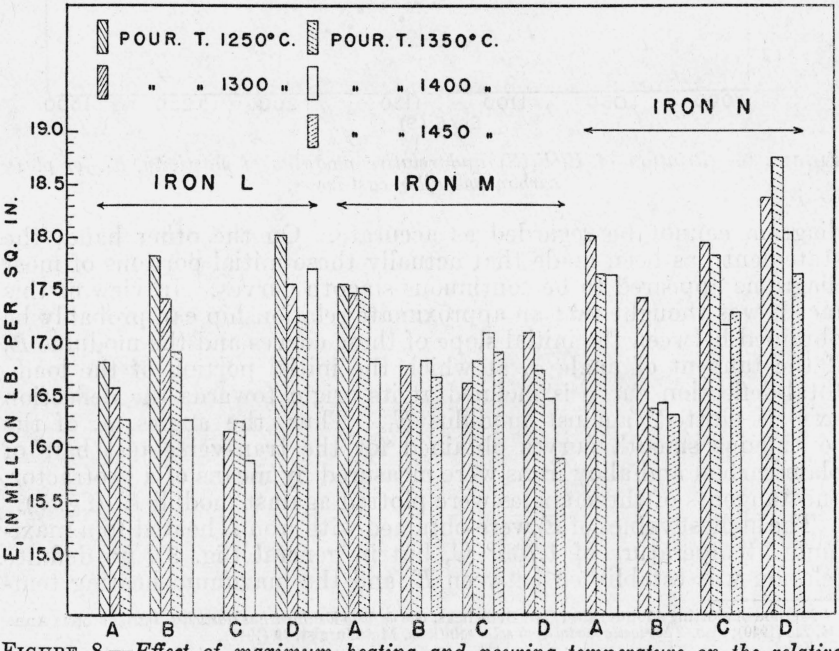

FIGURE 8.—*Effect of maximum heating and pouring temperature on the relative modulus of elasticity of irons L, M, and N.*

Maximum heating temperatures: *A*, 1,400° C; *B*, 1,500° C; *C*, 1,600° C; *D*, 1,700° C.

perature, whereas for the plain carbon irons there was a tendency for the values of E_1 to increase with increasing maximum heating temperature.

Effect of pouring temperature was practically the same for both alloy and plain carbon irons, that is, usually there was a decrease in E_1 values with increase in pouring temperatures. When comparing the moduli E_1 of alloy irons *L*, *M*, and *N* with those of plain carbon irons, it may be noted that moduli E_1 of alloy irons correspond to those of plain carbon iron *A*, heated to the maximum temperatures of 1,400°, 1,500°, and 1,600° C. However, the moduli of alloy irons are lower than moduli of iron *A* heated to maximum temperature of 1,700° C.

4. RESILIENCE

In agreement with common practice for cast iron, the term "resilience" is used in this paper to denote the work done in loading the specimen. The following resilience values are discussed below:

W_1=Ultimate total resilience obtained by measuring planimetrically the area below the load–total-deflection curve and between the origin and the ordinate drawn to the deflection curve at the point of rupture.

W_2=Ultimate triangular resilience, represented by a triangular area below a straight line drawn from the origin and the point of rupture on the load–total-deflection curve. It is obvious that triangular resilience only approximates the true resilience and that the degree of approximation decreases as the curvature of the load–total-deflection curve increases.

W_3=Ultimate elastic resilience was determined by calculating the triangular area below the ultimate elastic deflection curve on the assumption that this curve is a straight line. In view of the fact that ultimate elastic deflection curves deviate but slightly from a straight line, this assumption is permissible.

W_4=Ultimate plastic resilience. These resilience values were obtained by subtracting W_3 values from those of W_1.

The averages values of W_1 and W_4, as well as the ratios of W_4/W_1 expressed in percentage of W_1, for each group of bars cast at the same pouring temperature are shown in table 6. This table indicates that all these values are considerably lower for iron *L* than for irons *M* and *N*. The ultimate total-resilience values range as follows: for iron *L*, from 304 to 385 in.-lb; iron *M*, from 492 to 722 in.-lb; and iron *N*, 510 to 880 in.-lb. When drawing a comparison between alloy and plain carbon irons, it may be observed that plain carbon iron *A*, which showed total-resilience values from 220 to 375 in.-lb, approaches alloy iron *L*. Neither maximum heating nor pouring temperatures seem to have a considerable influence on these properties for irons *L* and *M*. However, a considerable improvement in these properties was observed for iron *N* when a lower range of pouring temperatures (1,300 to 1,350° C) was employed. When comparing all bars tested in this investigation, it may be noticed that iron *N* heated to the maximum temperature of 1,600° C and cast at pouring temperatures ranging from 1,300 to 1,350° C possessed the highest values of W_1 and W_4.

In connection with this observation it may be recalled that for plain carbon irons the effect of maximum heating and pouring temperatures was observed only for iron *A*, in which case there was a pronounced

TABLE 6.—*Resilience Values* [1]

Maximum heat temperature ° C		1,400			1,500			1,600			1,700		
Iron	Pouring temperature	Ultimate total resilience, W_1	Ultimate plastic resilience, W_4	Ratio W_4/W_1	Ultimate total resilience, W_1	Ultimate plastic resilience, W_4	Ratio W_4/W_1	Ultimate total resilience, W_1	Ultimate plastic resilience, W_4	Ratio W_4/W_1	Ultimate total resilience, W_1	Ultimate plastic resilience, W_4	Ratio W_4/W_1
	° C	*lb-in.*	*lb-in.*	*Percent*	*lb-in.*	*lb-in.*	*Percent*	*lb-in.*	*lb-in.*	*Percent*	*lb-in.*	*lb-in.*	*Percent*
L	1,400				341	73	21.41	311	56	18.00	335	70	20.90
	1,350	363	86	23.69				332	61	18.37	304	52	17.11
	1,300	379	89	23.48	328	67	20.43	385	81	21.04	372	75	20.16
	1,250	319	81	25.39	305	60	19.67				334	67	20.06
M	1,450				706	265	37.54	533	174	32.65	492	161	32.72
	1,400	581	191	32.87	603	217	35.99	612	215	35.13	528	167	31.63
	1,350	640	230	35.94				722	268	37.12	669	240	35.87
	1,300	659	242	36.72	692	253	36.56	557	190	34.11	592	198	33.45
	1,250	637	232	36.42									
N	1,450				510	131	25.69	644	189	29.35	581	153	26.33
	1,400	617	186	30.15	568	153	26.94	665	189	28.42	533	134	25.14
	1,350	619	189	30.53	608	168	27.63	880	277	31.48	751	205	27.30
	1,300	658	204	31.00	661	194	29.35	799	250	31.29	672	198	29.46

[1] Average values for each group of bars cast at the same pouring temperature.

decrease in resilience with increasing pouring temperatures. An increase in resilience with increasing maximum heating temperature was particularly evident in the bars of that iron poured at 1,350° C.

According to data compiled by Tucker [4], neither the breaking load, deflection, nor resilience values gave reliable indications of the resistance to thermal shock, but the plastic resilience, expressed in percentage of the total resilience, furnished a measure of the relative toughness of his irons. From this viewpoint, irons *M* and *N* should be more resistant to thermal shock than iron *L*. None of these irons, however, is superior, in this respect, to the plain carbon irons, previously examined. Actually all of them are inferior to a medium cylinder iron, *B*, whose plastic to total-resilience ratios ranged from 42 to 49 percent.

It is well known that silicon has a great effect on the physical properties of cast iron in general. In his work on the influence of phosphorus on iron, MacKenzie [5] plotted the ultimate total-deflec-

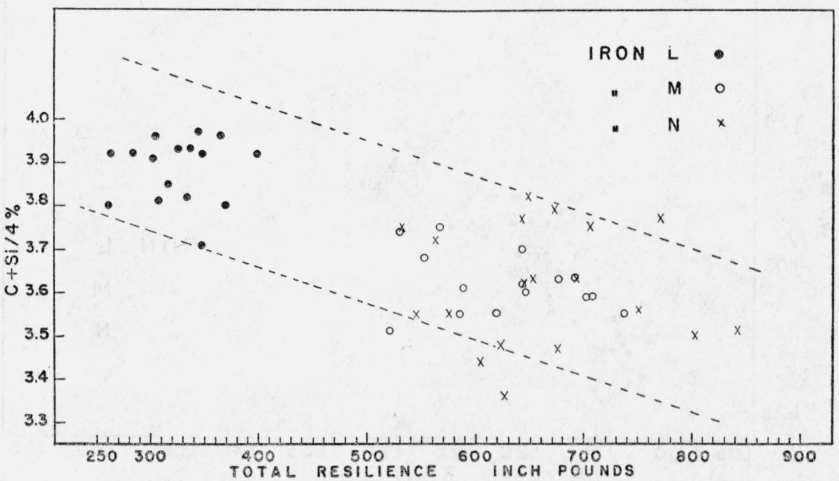

FIGURE 9.—*Relation of total resilience to carbon and silicon contents.*

tion values against the carbon content plus one-fourth of the silicon content and found that there was an increase of deflection with an increase of C+Si/4 values. His diagram indicated that deflection depends more on C+Si/4 values than on phosphorus content [6]. An attempt was made by the present writers in their previous paper [1] to find whether a corresponding relation to C+Si/4 content may be shown for the ultimate total-resilience values. Although a probable trend of the plotted points was outlined, it was found that the results obtained did not warrant any definite conclusion. In the present investigation, the values C+Si/4 for irons *L*, *M*, and *N* were plotted against W_1, W_3, and W_4. Although the plotted points are widely scattered, nevertheless, as may be seen in fig. 9, there is a definite trend for the ultimate total resilience to increase with a decrease of C+Si/4 values. A similar relation has been found for the ultimate plastic and elastic resiliences. Another interesting relation for the resilience values has been demonstrated by MacKenzie [7] for 1.2- by

18-in. bars tested transversely. The ratios of true resilience to triangular resilience were compared with ratios of modulus of elasticity at one-half load to ultimate modulus of elasticity. He showed that these ratios, when plotted in a logarithmic scale, were almost directly proportional to each other. It should be noted that in MacKenzie's experiments both modulus of elasticity at one-half load and ultimate modulus of elasticity were "secant moduli."

In the present investigation, the ratios $E_1(S)/E_2(S)$ were plotted (fig. 10) against ratios W_1/W_2 on linear scale; this gives roughly the

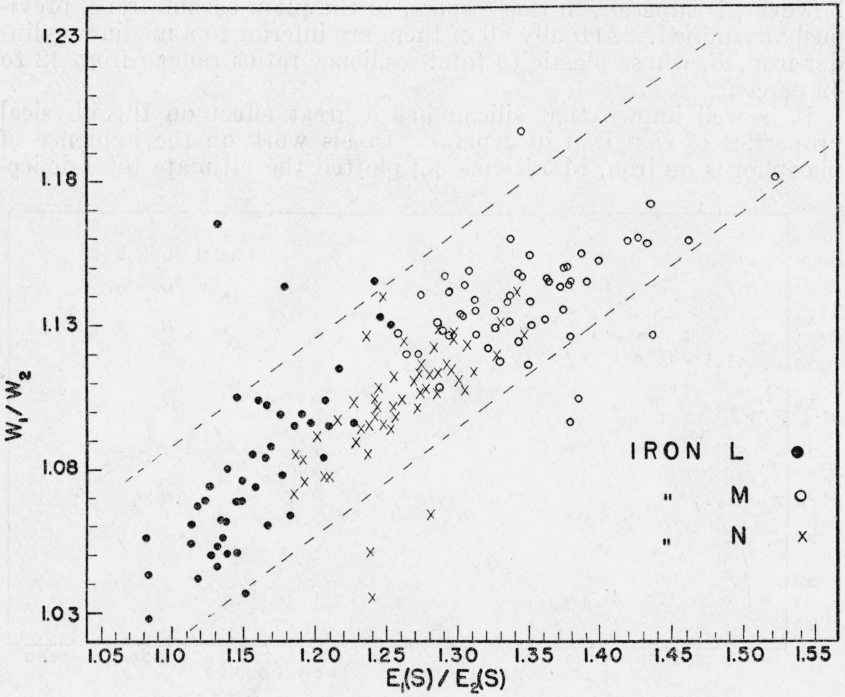

FIGURE 10.—*Relation of $E_1(S)/E_2(S)$ to W_1/W_2.*

same distribution of the points as a logarithmic plot, since the coordinates of the points are not far different from unity. Since E_2 is nearly equal to $E_1(S)$ (fig. 5), nearly the same relation was obtained for the ratios $E_1(S)/E_2(S)$ and $E_2/E_2(S)$. Both $E_1(S)/E_2(S)$ (fig. 10) and $E_2/E_2(S)$ tended to increase with increasing values of W_1/W_2.

5. HARDNESS

Brinell hardness numbers were determined on disks three-fourths inch thick cut from the tested transverse bars adjacent to the fracture. Three impressions were made on each disk; one near the center and two at points midway between the center and periphery. Two diameters were measured for each indentation, and the average of these six readings was used as the hardness number of a given specimen.

The Brinell numbers for the irons examined were as follows:

Iron *L*, 217 to 255.
Iron *M*, 255 to 269.
Iron *N*, 302 to 341.

No consistent relation was observed between the Brinell number and the transverse strength, maximum heating or pouring temperatures.

VI. MICROSCOPIC EXAMINATION

After the hardness was determined on one side of a disk, the opposite side (adjacent to the fracture) was ground, lapped on a lead-tin plate charged with fine emery, further lapped on a second plate charged with finer emery, and finally polished with an aqueous suspension of rouge, in an automatic polishing machine. Before final etching, the specimens were subjected to alternate polishing and etching operations. All the specimens were examined microscopically as polished and as etched with 1-percent solution of nitric acid in ethyl alcohol. The micrographs described below represent typical structures of the irons.

Figure 11 indicates that of two transverse bars of iron *L* the bar possessing greater strength and hardness shows somewhat less ferrite, finer graphite, and more pronounced dendrites. The total and combined carbon contents for the stronger bars were 3.24 and 0.60 percent, respectively, and for the companion bar 3.34 and 0.56 percent. Molybdenum and nickel contents were around 0.75 and 1.05 percent, respectively. The austenite-pearlite transformation has not been suppressed. Both bars were poured at low temperatures. It is evident, therefore, that the difference observed in this case is an effect of the maximum heating temperature.

Figure 12 represents iron *M*. Here again, the finer graphite and more pronounced dendritic structures were associated with greater transverse strength. When etched and examined at lower magnification, this specimen exhibits long dendrites extending in a radial direction almost to the center of the specimen, the dendrites of the companion specimen being much shorter and fewer in number. The matrix of these specimens consists of coarse pearlite and the so-called "acicular structure" with islands of fine pearlite. It has been shown by various investigators [8, 9, 10] that an addition of molybdenum to cast iron reduces the rate of transformation of austenite and causes the appearance of a peculiar "acicular" structure. This structure has been called acicular pearlite, acicular troostite, or acicular ferrite. It may be also called "pseudomartensite." In subsequent discussion, this structure for convenience will be designated as "acicular" structure. Two inclusions (fig. 12, *D*), presumably "magnanese sulfide," apparently served as nuclei of the graphite formations within fine pearlitic areas.

In spite of a rather small difference between the mechanical properties of these two transverse test bars of iron *N*, a considerable difference was observed in their structures. Finer graphite globules and flakes are associated with a somewhat stronger bar (fig. 13, *C* and *D*). It may also be observed that the higher Brinell number and relative modulus of elasticity were obtained with the bar possessing larger graphite nodules. Both specimens exhibited dendritic structures. The grayish-white areas (fig. 13, *D*), representing the midribs and branches of the dendrites, appear at higher magnification (fig. 14, *C*) as austenite at the initial stage of its transformation. A spot showing laminar graphite surrounding small crystals of manganese sulfide (fig. 13, *D*) is of interest.

A large portion of the free carbon of the lower strength transverse test bar (fig. 13, *A* and *B;* fig. 14 *A* and *B*) is present in the form of globules, consisting of aggregates of small graphite flakes. In the middle of some of these globules the bluish-gray inclusions, presumably manganese sulfide, are plainly seen. A patch of eutecticlike graphite resembling the Widmanstätten structure and associated with globular and coarse flaky graphite is visible in figure 13 (*B*) and figure 14 (*A*).

Other interesting structural features are the graphite eutectic situated within a graphite globule in figure 14 (*B*) and the "fluffy" appearance of the edges of some graphite flakes shown in figures 13 (*B*) and 14 (*A*). The secondary graphite, that is, hypereutectoid and eutectoid graphite, is generally deposited on existing graphite flakes in the form of a smooth band which is similarly oriented to the main body and is therefore difficult to show. Sometimes, however, the secondary graphite is deposited on the graphite lamellae in an irregular manner, so that the edges have a "fluffy" appearance [11, 12].

With regard to Widmanstätten structures, Morrogh [11] believes that the grain size of the original austenite does not determine whether the graphite will be deposited normally or in Widmanstätten form, and the conditions favorable for the development of the graphite Widmanstätten pattern are a controlled rate of cooling, neither extremely slow nor extremely fast, and a eutectic graphite structure consisting of a few very coarse flakes. The actual rate of cooling required to produce this structure must be very critical, as the graphite Widmanstätten pattern is seen in a fully developed form only very rarely.

The chemical analysis and Brinell hardness of two test bars represented in figure 15 (*A*, *B*, *C*, and *D*) are practically the same, but their transverse strengths differ. The characteristic structural features of the higher strength bar (fig. 15, *C* and *D*) are globular and flaky graphite, well-developed dendritic pattern, free carbide, and a fine acicular structure. The lower strength bar of the same heat (fig. 15, *A* and *B*) contained globular and whorl-like formations of graphite, coarse acicular structure, and a small amount of fine pearlite. The dendritic pattern of this bar was less pronounced than that of the companion bar.

An interesting feature of the structure presented in figure 15 (*B*) is the inclusion of a perfect hexagonal form with the light twinning-like band in the middle. It appears that this inclusion has been moved during solidification from its original seat and slightly rotated. It has the appearance of a cube resting on one of its edges. Somewhat similar inclusions but without the light band in the middle were shown by Allen [13] and Ellis [14]. Both of these authors described it as a manganese sulfide crystal. Ellis, however, remarks that manganese sulfide crystals may not be pure manganese sulfide, but rather mixtures of sulfides.

It is known that manganese sulfide inclusions possess a cubic crystal structure and appear in cast iron as dove-gray colored crystals of square, triangular, trapezoidal, etc., form. In steel they are generally present as dove-gray colored globules. On the other hand, iron sulfide has a hexagonal crystal structure and is lighter [15] in color than manganese sulfide.

Whiteley [16] was able to show that at temperatures above the solidus the sulfide in steel consisted predominantly of iron sulfide.

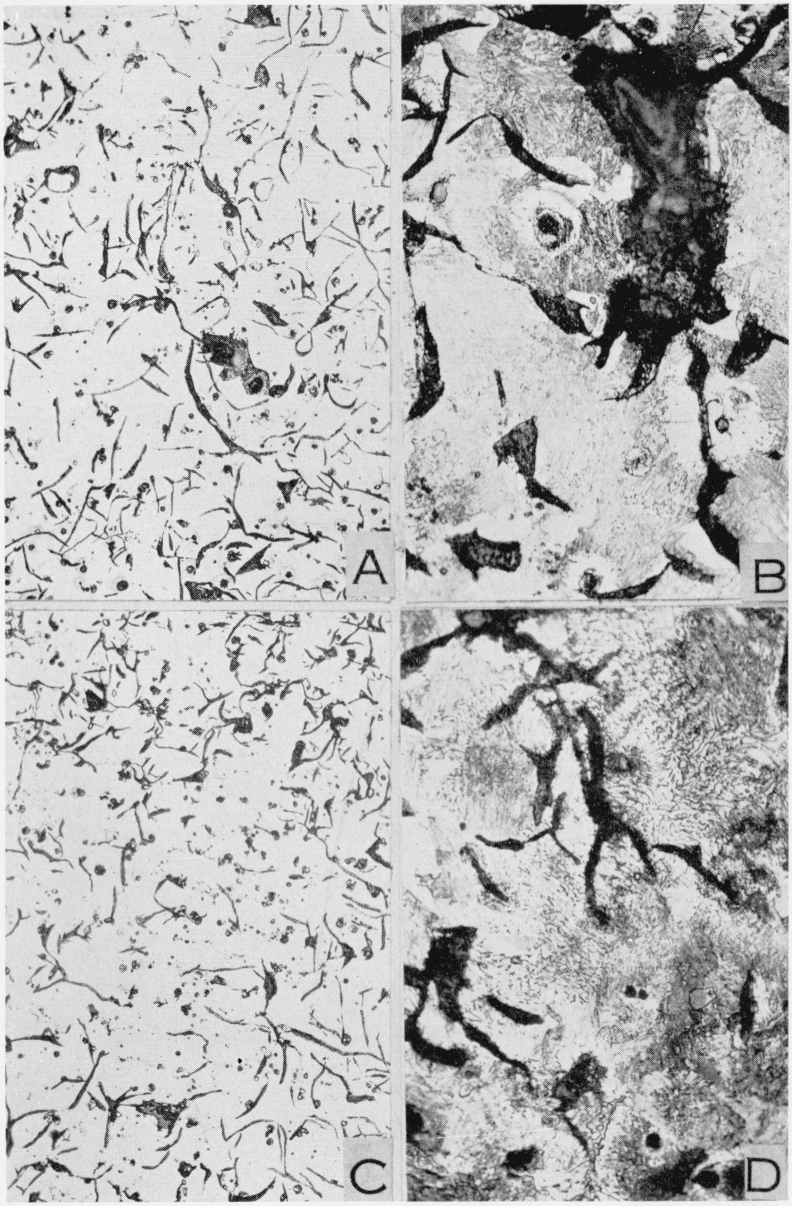

FIGURE 11.—*Iron L.*

Maximum temperature for *A* and *B*, 1,500° C; *C* and *D*, 1,700° C. Pouring temperature for *A* and *B*, 1,400° C; *C* and *D*, 1,300° C. Modulus of rupture for *A* and *B*, 61,000 lb/in.^{2}; *C* and *D*, 76,000 lb/in.^{2} $E_1 = 16 \times 10^6$ lb/in.^{2} for *A* and *B*. $E_1 = 17.7 \times 10^6$ lb/in.^{2} for *C* and *D*. Brinell hardness numbers for *A* and *B*, 229; *C* and *D*, 241. *A* and *C*, unetched, ×100; *B* and *D*, etched, ×500.

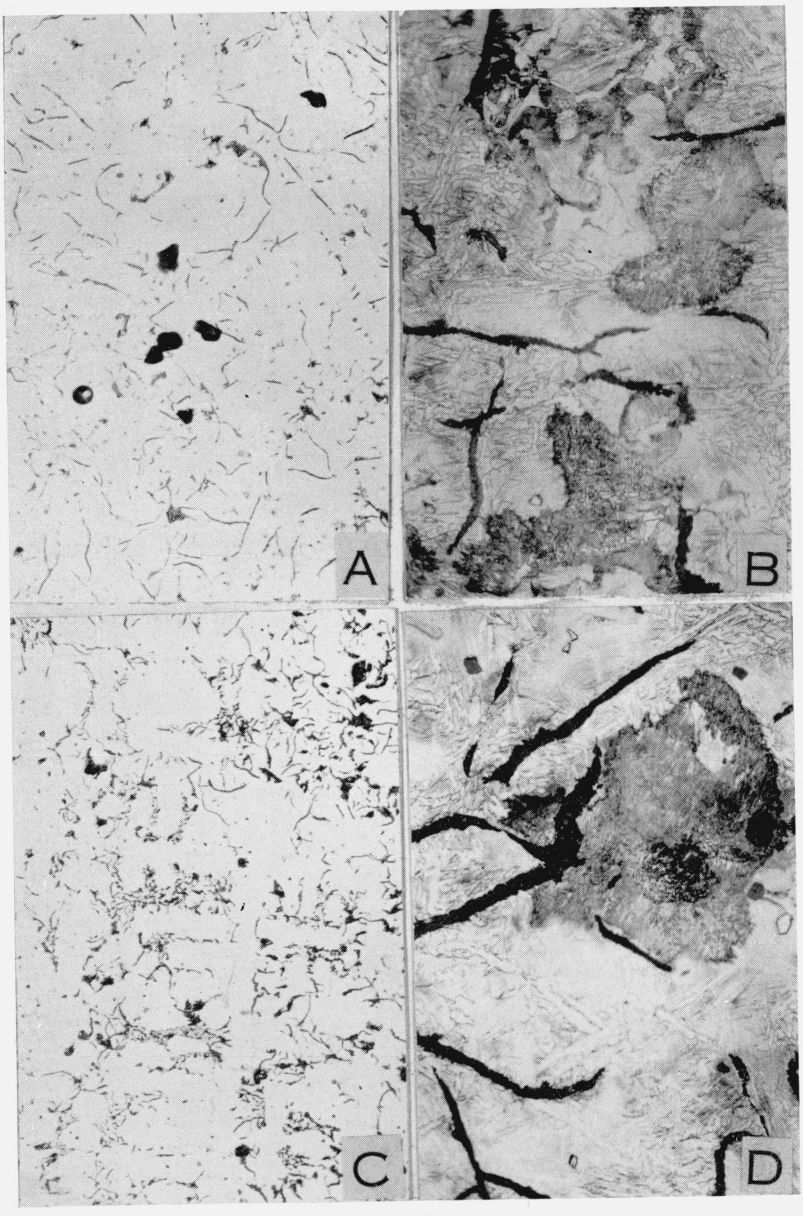

FIGURE 12.—*Iron M.*

Maximum temperature for *A* and *B*, 1,500° C; *C* and *D*, 1,600° C. Pouring temperature for *A*, *B*, *C*, and *D*, 1,350° C. Modulus of rupture for *A* and *B*, 78,000 lb/in.^{2}; *C* and *D*, 93,000 lb/in.^{2} $E_1=16.1\times10^6$ lb/in.^{2} for *A* and *B*. $E_1=17.0\times10^6$ lb/in.^{2} for *C* and *D*. Brinell hardness number for *A*, *B*, *C*, and *D*, 255. *A* and *C*, unetched, ×100; *B* and *D*, etched, ×500.

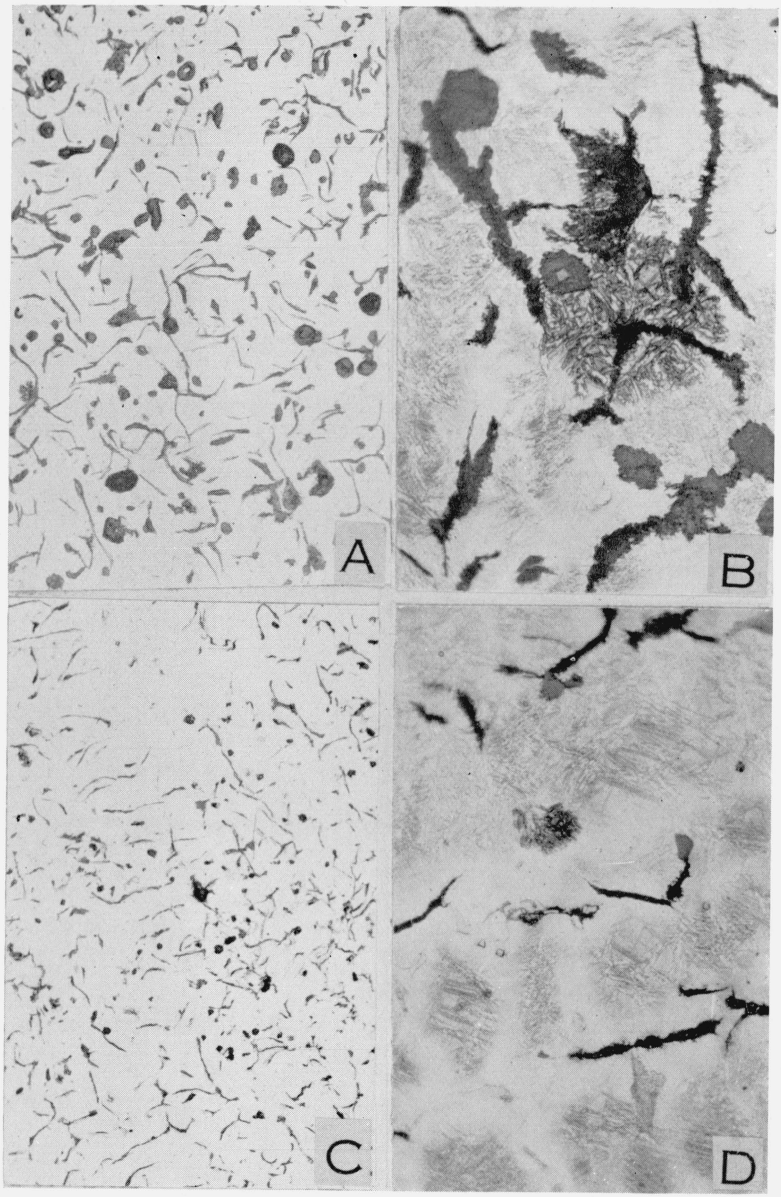

FIGURE 13.—*Iron N.*

Maximum temperature, 1,400° C. Pouring temperature for *A* and *B*, 1,400° C; *C* and *D*, 1,350° C. Modulus of rupture for *A* and *B*, 86,400 lb/in.^{2}; *C* and *D*, 99,300 lb/in.^{2} E_1=17.9×10^6 lb/in.^{2} for *A* and *B*. E_1=17.6×10^6 lb/in.^{2} for *C* and *D*. Brinell hardness numbers for *A* and *B*, 311; *C* and *D*, 302. *A* and *C*, unetched, ×100; *B* and *D*, etched, ×500.

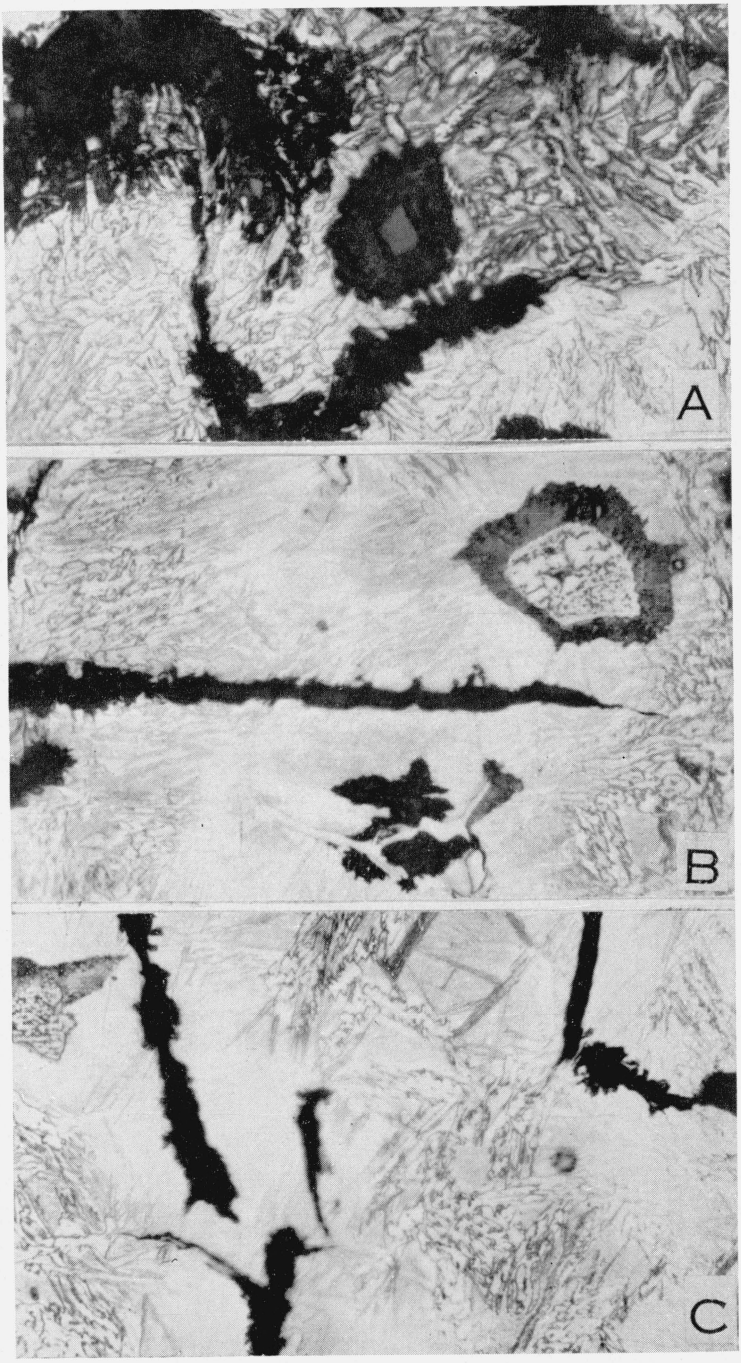

FIGURE 14.—*Iron N.*

A and *B* represent specimen shown in figure 13 (*A* and *B*), *C* represents specimen shown in figure 13 (*C* and *D*). Etched, ×1,500.

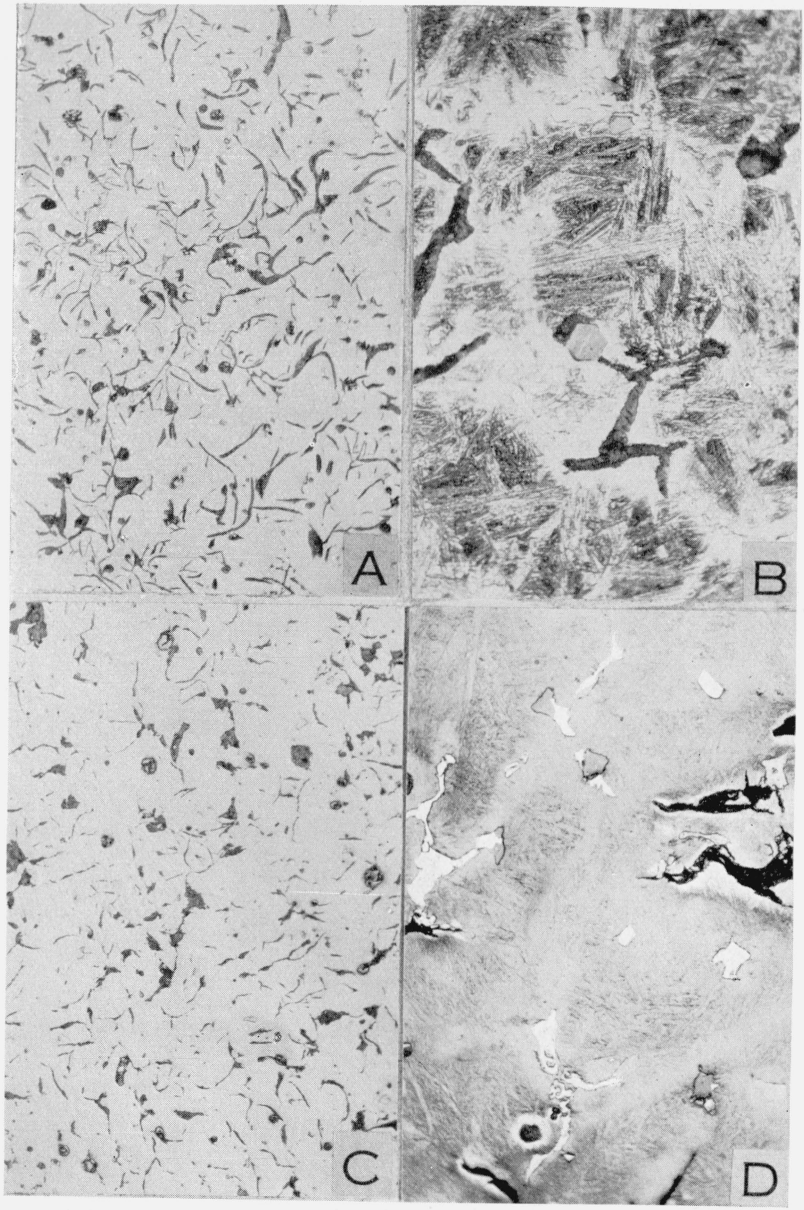

FIGURE 15.—*Iron N.*

Maximum temperature, 1,600° C. Pouring temperature for *A* and *B*, 1,450° C; *C* and *D*, 1,350° C. Modulus of rupture for *A* and *B*, 89,000 lb/in.^{2}; for *C* and *D*, 112,100 lb/in.^{2} E_1=17.3×10^6 lb/in.^{2} for *A* and *B*. E_1=18.7×10^6 lb/in.^{2} for *C* and *D*. Brinell hardness number for *A*, *B*, *C*, and *D*, 311. *A* and *C*, unetched, ×100; *B* and *D*, etched, ×500.

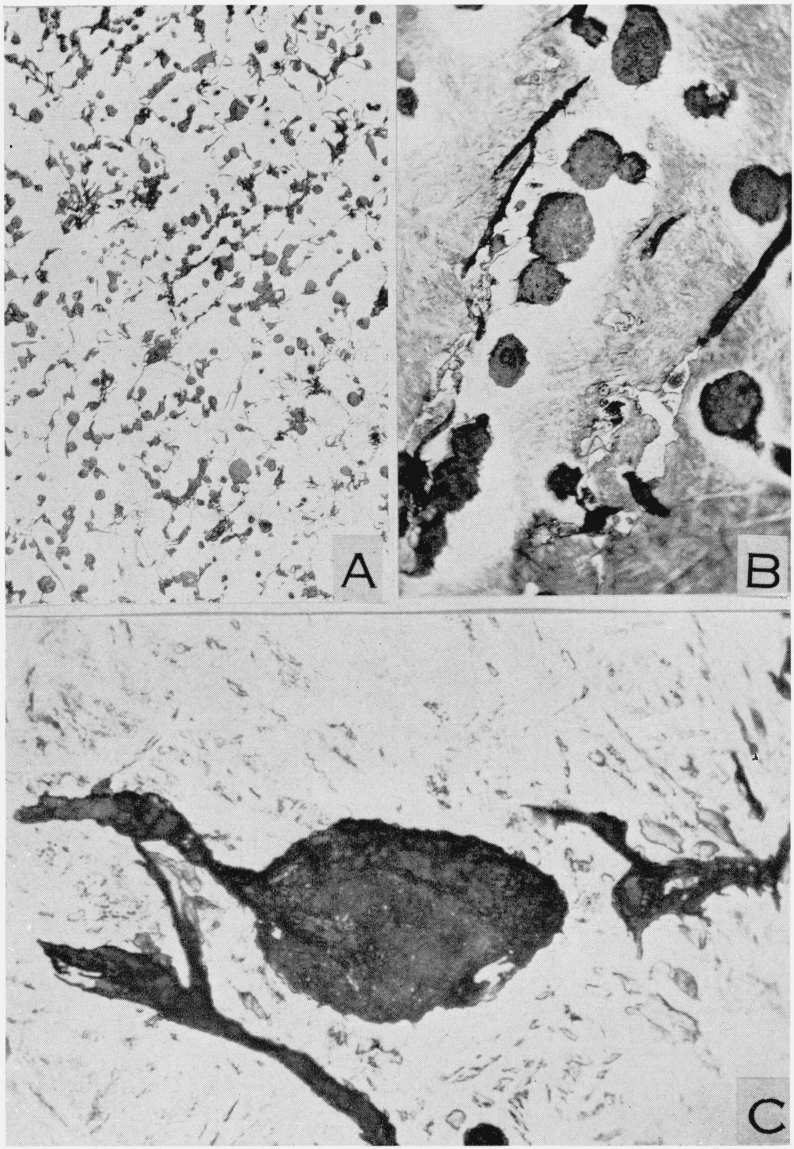

FIGURE 16.—*Iron N.*

Maximum temperature, 1,700° C. Pouring temperature, 1,350° C. Modulus of rupture, 104,000 lb/in.^{2} $E_1=18.60\times10.^6$lb/in^2. Brinell hardness number 341. *A*, unetched, ×100; *B*, etched, ×500; *C*, etched, ×1,500.

The appearance of iron sulfide at these temperatures is due to the fact that the reaction $FeS+Mn \rightleftharpoons MnS+Fe$ will tend to proceed toward the left at higher temperatures. At very drastic quenching from the liquid state, this investigator was able to show that FeS was present in liquid steel containing 0.06 percent of S and 0.6 percent of Mn. Iron sulfide may dissolve in the manganese sulfide.

Consideration of all of this evidence suggests that the inclusion shown in figure 15 (*B*) is probably a mixture of manganese and iron sulfides and that the light band in the middle is the remnant of iron sulfide proper.

In the middle portion of the flake, below the hexagonal inclusion just described (fig. 15, *B*), three dark lines crossing the flake at angles of about 60 degrees to its longitudinal axis may be noticed. These lines resemble the needles described by Hanemann and Schrader [17] and also by Morrogh [11]. They have shown that secondary graphite sometimes forms small needlelike crystals of different orientation from the graphite flake. If the flake is in its dark position, then the needles appear bright; and if the flake is in its bright position, the needles appear dark.

Figure 16 shows the structure of iron *N* heated to 1,700° *C* and poured at 1,350°C. The modulus of elasticity and Brinell hardness of this bar are about the highest obtained in the present investigation. It seems that most of the free carbon is present here in the form of globules (fig. 16, *A*). A row of graphite globules is shown in figure 16 (*B*). They have a spongy-like appearance, some of them being associated with graphite flakes, as may be seen in figure 16 (*C*). It appears as if they originated from the nucleus situated at the right end of the flake inside of the graphite nodule, but it is difficult to determine which of them, flake or globule, was formed first. If this globular graphite is of a temper-carbon nature, then the graphite flakes are eutectic graphite and the nodules are formed after solidification of the metal. Although the nodular formation of graphite is probably best developed in castings made from metal heated to 1,700° C, it cannot be stated that the high maximum heating temperature is responsible for such structure, because some nodular graphite was observed for the same iron, *N*, which had been heated only to 1,400° C and poured at 1,350° C (figs. 13, *A* and *B*). This structure is evidently characteristic for iron *N*, and seems to be a contributing factor in obtaining the higher values of the relative modulus of elasticity and Brinell hardness.

The structure of the matrix of the specimen in figure 16 (*B*) is acicular. The white area surrounding the graphite nodules when resolved at higher magnification (×1500) is shown in figure 16 (*C*). This structure resembles somewhat the micrographs presented by Davenport, Grange, and Hafsten [18] showing the initial and second stages of transformation of coarse-grained austenite at 540°C.

Microscopic examination indicates that a pearlitic matrix with the presence of some ferrite is responsible for the low strength of iron *L* as compared with irons *M* and *N*. The relatively low strength and Brinell hardness of iron *M* as compared with iron *N* may be caused by some pearlite in its structure. Acicular structure and fine graphite are associated with high strength in the irons examined. Iron *N* possessed large graphite globules and fine acicular matrix and had the highest Brinell number. In general, the globular formation of graphite seems to be a contributing factor in obtaining high values of relative modulus of elasticity and Brinell hardness.

It was found, when examining test bars of the same heat, that the bars possessing greater strength showed a pronounced dendritic pattern. Since it is commonly accepted that random distribution of graphite particles produces stronger cast iron than does dendritic structure, it may be inferred that the high strength bars showing dendritic patterns would possess still greater strength if their graphite particles were arranged at random.

VII. SUMMARY

1. The mechanical properties of three alloy irons (*L*, a nickel-molybdenum iron; *M* a nickel-molybdenum-chromium, low-manganese, medium-silicon iron; and *N*, a nickel-molybdenum-chromium, high-manganese, high-silicon iron) were determined by measurements under transverse loading.

2. The average transverse strength, ultimate total and elastic deflections, resilience, and Brinell hardness of irons *M* and *N* were found to be superior to those of iron *L*.

3. The maximum heating temperature showed no effect on the transverse strength of irons *L* and *M*, but the moduli of rupture of iron *N* were somewhat higher for the maximum heating temperatures of 1,600° and 1,700° C than for 1,400° and 1,500° C. The highest moduli of elasticity of all the bars tested were obtained with iron *N* at the heating temperature at 1,700° C, but in general no definite relation could be established between the relative moduli of elasticity and the maximum heating temperature. The lower pouring temperatures, ranging from 100° to 150° C above the liquidus, tended to increase the strength and relative modulus of elasticity of the irons examined. Neither maximum heating nor pouring temperatures exerted much influence on the resilience values for irons *L* and *M*, but a considerable improvement in these properties was observed for iron *N* when a lower pouring temperature was employed.

4. The elastic-deflection curves of the alloy irons studied in this investigation were similar to those of the plain carbon irons described in the previous paper, that is, they were straight lines in their lower portion, but beginning at a certain point (approximately three-fifths of the breaking load), they inclined toward the deflection axis.

5. Four relative moduli of elasticity were determined: E_1, calculated from the lower portion of the elastic-deflection curve; $E_1(S)$, secant modulus corresponding to the load at which E_1 was calculated; E_2, ultimate modulus computed from the elastic-deflection curve at the breaking point; and $E_2(S)$, ultimate secant modulus at the breaking load. The values of these moduli decreased in the following order: E_1, E_2, $E_1(S)$ and $E_2(S)$. There was a rather small difference between E_1, E_2, and $E_1(S)$ values, but $E_2(S)$ was considerably lower.

6. The ratios of the average ultimate plastic resilience, W_4 (the area below the load–plastic-deflection curve between the origin and the ordinate drawn to the plastic-deflection curve at the point of rupture), and ultimate total resilience, W_1 (area below the load–total-deflection curve and between the origin and the ordinate drawn to the total deflection curve at the point of rupture), were considerably higher for irons *M* and *N* than for iron *L*.

7. There is a definite trend for the ratios $E_1(S)/E_2(S)$ and $E_2/E_2(S)$ to increase with an increase of ratio W_1/W_2, where W_1 is the ultimate

total resilience and W_2 the ultimate triangular resilience, represented by a triangular area below a straight line drawn from the origin to the point of rupture on the load–total-deflection curve.

8. Comparison of alloy irons *L*, *M*, and *N* with plain carbon irons *A*, *B*, and *C* previously investigated indicates that:

(a) Iron *A*, showing higher strength, elasticity, and resilience values than companion plain carbon irons, possesses strength and resilience equivalent to those of a nickel-molybdenum iron.

(b) The relative moduli of elasticity of iron *A* heated to the maximum temperature of 1,700° C are higher than those of alloy irons.

(c) The beneficial effect of the maximum heating temperature on the moduli of rupture and elasticity was more pronounced for the plain carbon irons than for alloy irons. The effect of pouring temperature for both plain carbon and alloy irons, was about the same, that is, these properties showed a tendency to increase with a decrease in pouring temperature.

(d) The plastic to total resiliences ratios of plain carbon iron *B* (a medium cylinder iron) are higher than those of alloy irons.

(e) If the proportion of plastic deflection to the total deflection at fracture is accepted as an index of plasticity of cast iron, an alloy iron, *L*, may be considered as being the most rigid and plain carbon iron *B* the least rigid.

9. The structure of iron *L* consists of flaky graphite and pearlite. The matrix of irons *M* and *N* appears to be made up of the transition product of austenite, an "acicular" structure.

10. The graphite of iron *N* shows a tendency to form globules. This was particularly pronounced in the specimen of this iron when heated to the maximum temperature of 1,700° C and poured at 1,350° C. It is probable that the nodular graphite structure is a contributing factor in obtaining the higher values of the relative modulus of elasticity and Brinell hardness. Some unusual structures of iron *N* were observed, and a tentative explanation was offered for the following: a patch of a eutecticlike graphite resembling the Widmanstätten pattern; the fluffy appearance of the edges of some graphite flakes; an inclusion, presumably manganese sulfide, of a perfect hexagonal form with the light twinninglike band in the middle; and the dark lines observed on a graphite flake and crossing it at about a 60-degree angle.

Grateful acknowledgement is made to L. D. Jones and Houston Babb for assistance in this investigation.

VIII. REFERENCES

[1] A. I. Krynitsky and C. M. Saeger, Jr., *Elastic properties of cast iron*, J. Research NBS **22,** 191 (1939) RP1176.

[2] A. I. Krynitsky and C. M. Saeger, Jr., *An improved method for preparing cast iron transverse test bars*, J. Research NBS **16,** 367 (1936) RP880.

[3] A. I. Krynitsky and C. M. Saeger, Jr., *New method of measuring deflection in the transverse-loading test of cast iron*, Bul. Am. Soc. Testing Materials, No. 97, 23 (1939).

[4] R. C. Tucker, *Pig iron*, Foundry Trade J. **56,** 347 (1937).

[5] J. T. MacKenzie, *The influence of phosphorus on iron*, Trans. Am. Foundrymen's Assn. **33,** 445 (1925).

[6] J. W. Bolton, Gray cast iron (The Penton Publishing Co., Cleveland, O., 1937).
[7] J. T. MacKenzie, *Report of Subcommittee 15 on Impact Testing*, Proc. Am. Soc. Testing Materials **33,** pt. 1, 87 (1933).
[8] G. A. Timmons, V. A. Grosby, and A. J. Herzig, *Produces high strength iron*, Foundry **66,** No. 12, 28 (1938); **67,** No. 1, 30 (1939).
[9] R. A. Flinn and D. J. Reese, The Development and Control of Engineering Gray Cast Irons, Preprint, Am. Foundrymen's Assn. (1941).
[10] C. A. Nagler and R. L. Dowdell, Heat Treatment of Cast Iron, Preprint, Am. Foundrymen's Assn. (1941).
[11] H. Morrogh, The Polishing of Cast Iron Microspecimens and the Metallography of Graphite Flakes, Preprint, Iron & Steel Inst. (May 5, 1941).
[12] H. Hanemann and A. Schrader, Atlas Metallographicus, **2,** No. 3, Plate 23, Figs. 161–163 (Gebrüder Bornträger, Berlin, 1936).
[13] R. M. Allen, *The microscope as a practical aid in the cast iron foundry*, Trans. Am. Foundrymen's Assn. **39,** 733 (1931).
[14] O. W. Ellis, *Crystalline manganese sulphide in chilled cast iron*, Metals & Alloys, **8,** 221 (1937).
[15] H. Morrogh, *Metallography of inclusions in cast iron and pig irons*, Foundry Trade J. **64,** 37 (1941).
[16] J. H. Whiteley, Seventh Report on the Heterogeneity of Steel Ingots, Iron & Steel Inst., Section IIIA, **23** (1937).
[17] H. Hanemann and A. Schrader, Atlas Metallographicus, **2,** No. 1, Plate 3, Fig. 27 (Gebrüder Bornträger, Berlin, 1936).
[18] E. S. Davenport, R. A. Grange, and R. F. Halsten, *Influence of austenite grain size upon isothermal transformation behavior of SAE 4140 steel*, Metals Tech. (Am. Inst. Min. Engrs.) **8,** No. 1, Tech. Pub. No. 1276 (1941).

WASHINGTON, October 3, 1941.